

# An Efficient Continuous-Time MILP for Integrated Aircraft Hangar Scheduling and Layout

Shayan Farhang Pazhooh<sup>1</sup><sup>a</sup>, Hossein Shams Shemirani<sup>2</sup><sup>b,\*</sup>

<sup>a</sup>*Department of Industrial Engineering, Isfahan University of Technology, Isfahan, Iran*  
<sup>b</sup>*Industrial Engineering Group, Golpayegan College of Engineering, Isfahan University of Technology, Golpayegan 87717-67498, Iran*

---

## Abstract

Efficient management of aircraft maintenance hangars is a critical operational challenge, involving complex, interdependent decisions regarding aircraft scheduling and spatial allocation. This paper introduces a novel continuous-time mixed-integer linear programming (MILP) model to solve this integrated spatio-temporal problem. By treating time as a continuous variable, our formulation overcomes the scalability limitations of traditional discrete-time approaches. The performance of the exact model is benchmarked against a constructive heuristic, and its practical applicability is demonstrated through a custom-built visualization dashboard. Computational results are compelling: the model solves instances with up to 25 aircraft to proven optimality, often in mere seconds, and for large-scale cases of up to 40 aircraft, delivers high-quality solutions within known optimality gaps. In all tested scenarios, the resulting solutions consistently and significantly outperform the heuristic, which highlights the framework's substantial economic benefits and provides valuable managerial insights into the trade-off between solution time and optimality.

*Keywords:* Aircraft Maintenance, Hangar Scheduling, Spatial-Temporal Optimization, Mixed-Integer Linear Programming, Heuristic Algorithm, Decision Support Systems

---

\*Corresponding Author

Email addresses: [shayanfp2006@gmail.com](mailto:shayanfp2006@gmail.com) (Shayan Farhang Pazhooh<sup>1</sup>), [h.shams@iut.ac.ir](mailto:h.shams@iut.ac.ir) (Hossein Shams Shemirani<sup>2</sup>)

## 1. Introduction

The global aircraft maintenance, repair, and overhaul (MRO) market is a multi-billion dollar industry in which operational efficiency directly translates to profitability. Within this complex ecosystem, the maintenance hangar emerges as a pivotal yet capacity-constrained asset, often serving as a critical bottleneck in the MRO value chain. Consequently, optimizing hangar space and time utilization presents a paramount challenge for airlines and service providers, with direct implications for fleet readiness (i.e., the availability of aircraft for scheduled operations) and financial performance.

The hangar scheduling problem represents a complex spatial-temporal optimization challenge, falling within the broader class of Operations Routing and Scheduling Problems (ORSP) that integrate logistical movements with operational tasks (Jiang et al., 2025). It involves two intertwined subproblems: a temporal scheduling problem (when to bring aircraft in and out) and a spatial allocation problem (where to park them). Decisions made in one domain directly constrain the other. For instance, the physical placement of one aircraft can block the movement of another, dictating the sequence in which they must depart. Similarly, the scheduled arrival and departure times determine which aircraft must share the hangar space simultaneously, thus constraining the possible spatial layouts.

While this complex problem has been addressed in the literature, existing exact methods often rely on computationally intensive discrete-time formulations. A prominent example is the work of Qin et al. (2019), who, recognizing the severe scalability limitations of basic discrete-time models, developed a significantly more efficient event-based reformulation. This enhanced model performed remarkably well in many scenarios, solving some instances with up to ten aircraft to optimality in mere seconds. However, its performance remains sensitive to problem characteristics beyond the number of aircraft. In one particularly challenging instance—featuring only nine aircraft but highly congested arrival times—the model failed to find an optimal solution within a one-hour time limit. This example highlights that even advanced formulations can struggle under operational complexity, necessitating the use of heuristics such as rolling horizon approaches, which inherently sacrifice guarantees of global optimality.

This paper aims to overcome these limitations by introducing a novel and efficient continuous-time MILP formulation. The main contributions of this work are threefold:

1. **A Novel Continuous-Time Formulation:** We propose an efficient MILP model that treats time as a continuous variable. This approach fundamentally reduces the model's complexity, including the number of variables and constraints, compared to discrete-time counterparts, enabling the efficient solution of larger and more realistic problem instances.
2. **A Comprehensive Computational Study:** We benchmark the performance of our exact model against a fast, priority-rule-based constructive heuristic, quantifying the significant economic value of achieving optimality.
3. **An Insight-Driven Decision Support Framework:** We present a custom-built visualization tool that transforms the model's numerical output into an interactive dashboard. This framework serves as a powerful analytical instrument, enabling managers to explore the optimal plan and, crucially, understand the complex rationale behind the model's strategic decisions, thereby bridging the gap between advanced analytics and operational execution.

Collectively, this research provides a holistic and scalable framework for optimizing hangar operations, leading to improved throughput, reduced costs, and significant managerial insights.

## 2. Literature Review

The optimization of maintenance activities is a well-established field in operational research, with a vast body of literature dedicated to developing models that enhance efficiency and reliability across various industries (de Jonge and Scarf, 2020; Arts et al., 2025). Within this broad domain, aircraft maintenance presents a unique set of challenges due to the high value of assets, stringent safety regulations, and the complex interplay of operational constraints. Research in aircraft maintenance spans multiple decision levels, from strategic fleet-wide planning—such as maximizing fleet availability (Gavranis and Kozanidis, 2015), maintenance routing (Sriram and Haghani, 2003; Qin et al., 2024), and long-term check scheduling (Andrade et al., 2021)—to tactical resource allocation, including personnel rostering (Belien et al., 2012) and technician assignment (Chen et al., 2017). Our work is situated at the operational core of MRO activities: the aircraft hangar scheduling

problem, which lies at the intersection of scheduling, layout planning, and packing problems. This paper addresses the operational-level decision of assigning precise roll-in/out times and physical parking positions for incoming aircraft, considering spatial and temporal constraints.

The development of exact models for this problem has evolved from static, single-period spatial allocation to dynamic, multi-period scheduling. An early key work by Qin et al. (2018) addressed the static aircraft parking stand allocation problem, focusing on maximizing profits and safety margins for a single day by selecting a subset of aircraft. This was extended into a comprehensive, multi-period model by Qin et al. (2019), which presents an integrated mathematical model for the hangar scheduling and layout problem. Their work is comprehensive, addressing both temporal and spatial dimensions with detailed considerations for aircraft geometry and movement blocking. However, their formulation is based on a discrete-time framework, where decision variables are indexed by specific time points. While this method is conceptually straightforward, it suffers from significant scalability issues. As the authors note, their model struggles to find optimal solutions for instances with as few as 9 aircraft within a one-hour time limit, necessitating a rolling horizon approach for larger, more realistic instances, which sacrifices global optimality. This computational burden is well-documented in discrete-time models, as demonstrated in the multi-period hangar scheduling formulation of Qin et al. (2019).

The core challenge of the hangar problem—managing high-value assets through a capacitated, shared transfer system—is not unique to aviation. A strong parallel exists in the maritime industry with syncrolift dry dock scheduling, where ships are moved between the sea and onshore service bays via a shared lift and railway system. Guan et al. (2025) address this by developing an MILP model to minimize ship waiting times, explicitly modeling the transfer system as a series of capacity-constrained segments. Their work underscores the critical role of the transfer system as a bottleneck and highlights the value of integrated scheduling, reinforcing the general importance of the problem structure we address. To overcome the scalability limitations of exact models, other approaches have emphasized different facets of the hangar scheduling problem. Recognizing the problem’s similarity to two-dimensional irregular packing, Niu et al. (2025) developed a two-stage metaheuristic framework to maximize hangar utilization. Others have viewed it as a variant of the bin packing problem, as seen in the work of Witteman et al. (2021), who modeled maintenance task allocation.

The trend towards more realistic and integrated models increasingly situates specific operational problems within the broader airport ecosystem. For instance, significant research has focused on optimizing other critical airport bottlenecks, such as runway operations through collaborative flight scheduling (Jiang et al., 2024) and ground-side efficiency via the scheduling of autonomous electric vehicles for baggage transport (Zhang et al., 2025). While these studies are vital for overall airport performance, our work addresses the maintenance hangar—a vital and distinct component of airport logistics with its own unique set of spatial-temporal challenges.

Separately, other models have advanced the state-of-the-art in hangar planning by incorporating more realism. These include combining hangar scheduling with multi-skilled technician assignment (Qin et al., 2020), addressing task rescheduling in disruptive environments (van Kessel et al., 2023), and using stochastic scheduling to account for uncertain aircraft utilization and maintenance durations (Deng and Santos, 2022). While these models are valuable for capturing operational complexities, they often rely on heuristics or inherit the computational challenges associated with their underlying discrete-time or event-based structures.

This review of the literature reveals a clear research gap: the need for an exact and scalable formulation for the integrated hangar scheduling problem. Existing models often face computational limitations, particularly under conditions of high temporal congestion, forcing a reliance on heuristics that sacrifice global optimality. This paper directly addresses this gap by proposing a novel continuous-time MILP model. This approach represents a fundamental shift from discrete-time or event-based frameworks, significantly reducing model complexity and enhancing computational efficiency. Our model is further distinguished by its comprehensive cost structure, including arrival delay penalties, and its ability to handle initial hangar states. By providing a robust and scalable exact method, benchmarked against a custom heuristic and supported by a practical visualization tool, our work offers a powerful framework for optimizing real-world MRO operations.

### 3. Problem Definition and Mathematical Model

The problem is formulated as a mixed-integer linear program (MILP). The following sections detail the sets, parameters, and variables that define the model, followed by an in-depth explanation of the objective function and constraints.

### 3.1. Problem Definition and Assumptions

The problem addressed in this paper is the integrated scheduling and spatial allocation of aircraft within a maintenance hangar. The objective is to determine which new aircraft to accept, when they should arrive and depart, and where they should be parked to minimize total operational costs, which include penalties for rejections and delays.

The operational environment is defined by the following key assumptions, which form the basis for our mathematical model:

- **Hangar Layout and Access:** We model the hangar as a rectangular area with a single, primary entrance/exit located along the edge corresponding to the highest Y-coordinates. This "open-front" configuration, which is consistent with modern, large-span hangar designs that favor a wide layout for structural integrity and operational efficiency (Liu et al., 2025), dictates that all aircraft movements are sequential and primarily oriented along the Y-axis.
- **Movement Exclusivity:** To prevent logistical conflicts and ensure safety, no two movement events (i.e., an aircraft rolling in or rolling out) can occur simultaneously. A minimum time gap, denoted by  $\varepsilon_t$ , must be maintained between any two consecutive movements. This is enforced through a set of temporal separation constraints within the mathematical model.
- **Aircraft Geometry and Buffer:** Each aircraft is represented by its rectangular footprint  $(W_a, L_a)$ . A mandatory safety 'Buffer' must be maintained between all aircraft and, crucially, between aircraft and the hangar walls. This dual application of the buffer is vital: the aircraft-to-aircraft buffer ensures safe separation, while the aircraft-to-wall buffer provides essential clearance for personnel and ground-based maintenance equipment (e.g., mobile lifts, hydraulic platforms), ensuring safe maintenance access while mitigating the risk of collisions and scratches, a factor identified as a critical source of danger in recent hangar scheduling models (Liu et al., 2023). In contrast to more complex geometric approaches like the no-fit polygon (NFP) method used in some literature (Qin et al., 2018, 2019), this simplification is justified by operational reality. The space enforced by a rectangular bounding box is practically necessary to accommodate maintenance equipment,

allow for tasks such as opening engine cowlings, and ensure safe passage for technicians. While NFP could theoretically achieve a denser packing, the use of buffered rectangles provides a realistic and computationally tractable representation of the required operational space.

- **Static Placement:** Once an aircraft is parked in the hangar, its position is considered fixed until its scheduled departure. The model does not account for the repositioning or shuffling of aircraft during their maintenance stay. This assumption significantly simplifies the model but also aligns with operational practice, where repositioning an aircraft is a complex, time-consuming, and costly procedure that is generally avoided. By creating a stable plan, this assumption enhances predictability. Incorporating dynamic repositioning capabilities remains a viable and interesting avenue for future research.

### 3.2. Sets and Indices

Sets are used to group the main entities in our model. We define three primary sets to categorize the aircraft.

- $a, b \in A$ : This is the universal set of all aircraft involved in the planning horizon. It is the union of aircraft already in the hangar and new aircraft requesting service ( $A = C \cup F$ ).
- $c, d \in C$ : This set represents the **current** aircraft that are already inside the hangar at the start of the planning period ( $C \subset A$ ). These aircraft have fixed initial positions and remaining service times.
- $f, g \in F$ : This set includes all **future** (new) aircraft that have requested hangar space for maintenance ( $F \subset A$ ). The model will decide whether to accept or reject these requests.

### 3.3. Scalars

Scalars are constant values that define the physical and operational environment of the model.

- $HW, HL$ : These represent the total interior **width** and **length** of the hangar, respectively. They define the boundaries of the available parking area.

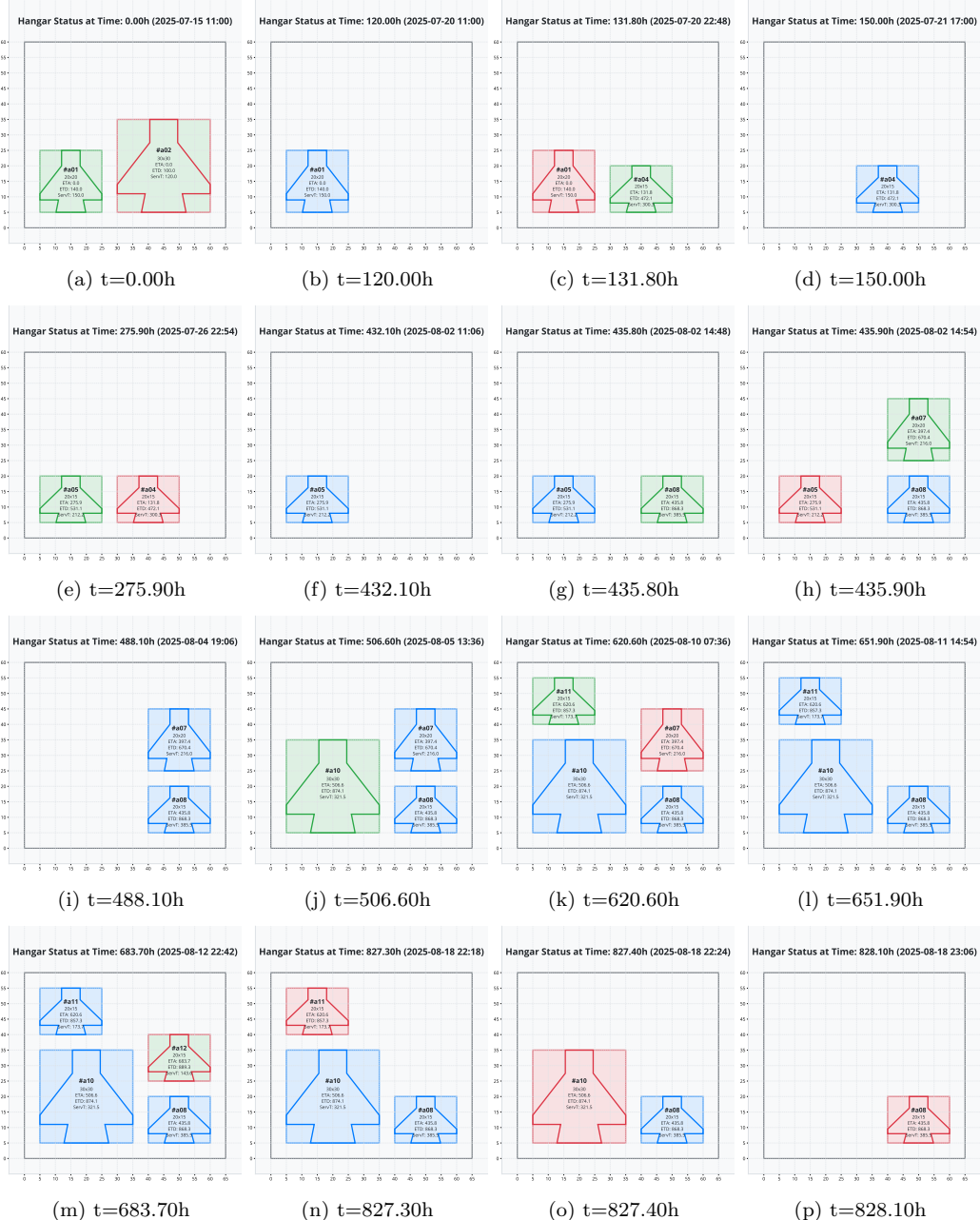


Figure 1: The complete temporal evolution of the hangar configuration for the N10 test instance, based on the optimal MILP solution. The progression shows the hangar's state at each key event, from start to finish, illustrating the sequence of arrivals and departures. Aircraft colors indicate their status: static (blue), arriving (green), or pre-departure (red).

- *Buffer*: This scalar specifies the minimum required safety distance that must be maintained between any two aircraft, and between an aircraft and the hangar walls. This is crucial for safe movement and operations.
- $M_T, M_X, M_Y$ : These are sufficiently large positive constants, commonly known as "Big-M" values, used in mathematical programming to activate or deactivate constraints. Their values are set dynamically based on the problem's dimensions to ensure they are sufficiently large for any given instance, which preserves the model's scalability.
  - $M_T = \max_{f \in F}(ETA_f) + \sum_{a \in A}(ServT_a)$ : A large time constant, calculated as the latest arrival time plus the sum of all service times. It is guaranteed to be larger than any possible roll-in or roll-out time in the model.
  - $M_X = HW$ : A large distance constant equal to the hangar width.
  - $M_Y = HL$ : A large distance constant equal to the hangar length.
- $\varepsilon_t$ : A small time value representing the minimum required interval between consecutive aircraft movements (arrivals or departures) to prevent logistical conflicts.
- $\varepsilon_p$ : A small penalty coefficient used in the objective function to encourage the model to place new aircraft closer to the origin (0,0), promoting a tidy and consolidated layout.

### 3.4. Parameters

Parameters are input data specific to each aircraft.

- $W_a, L_a$ : The **width** and **length** of aircraft  $a$ . These define the rectangular footprint of each aircraft.
- $ETA_a, ETD_a$ : The **Expected Time of Arrival** and **Expected Time of Departure** for aircraft  $a$ . These are the target times based on the initial schedule.
- $ServT_a$ : The required **service time** for aircraft  $a$ . For current aircraft ( $c \in C$ ), this is the *remaining* service time.

- $P_f^{Rej}, P_f^{Arr}, P_a^{Dep}$ : These are the penalty costs.  $P_f^{Rej}$  is the cost incurred if we **reject** a new aircraft  $f$ .  $P_f^{Arr}$  is the per-unit-time cost for an **arrival delay** of aircraft  $f$ .  $P_a^{Dep}$  is the per-unit-time cost for a **departure delay** of aircraft  $a$ .
- $X_c^{init}, Y_c^{init}$ : The fixed initial X and Y coordinates of current aircraft  $c$ , which are already in the hangar.

### 3.5. Decision Variables

Decision variables are the outputs of the model; their values are determined by the solver to achieve the optimal solution.

#### 3.5.1. Continuous Variables

- $X_a, Y_a$ : The X and Y coordinates of the front-left corner of aircraft  $a$ . These variables determine the exact placement of each aircraft in the hangar.
- $Roll\_in_a, Roll\_out_a$ : The actual **roll-in** (entry) and **roll-out** (exit) times for aircraft  $a$ .
- $D_f^{Arr}, D_a^{Dep}$ : The calculated **arrival delay** for new aircraft  $f$  and **departure delay** for any aircraft  $a$ .

#### 3.5.2. Binary Variables

- $Accept_a$ : A binary flag that is 1 if aircraft  $a$  is accepted for service, and 0 otherwise. For current aircraft ( $c \in C$ ), this is fixed to 1.
- $Right_{ab}$ : 1 if aircraft  $a$  is positioned completely to the **right** of aircraft  $b$ , 0 otherwise.
- $Above_{ab}$ : 1 if aircraft  $a$  is positioned completely **above** (in the direction of increasing Y) aircraft  $b$ , 0 otherwise.
- $OutIn_{ab}$ : 1 if aircraft  $a$  rolls **out** before aircraft  $b$  rolls **in**.
- $InIn_{ab}$ : 1 if aircraft  $a$  rolls **in** before aircraft  $b$ .
- $OutOut_{ab}$ : 1 if aircraft  $a$  rolls **out** before aircraft  $b$ .
- $InOut_{ab}$ : 1 if aircraft  $a$  rolls **in** before aircraft  $b$  rolls **out**.

### 3.6. Objective Function

The objective is to minimize the total operational cost  $Z$ , which is formulated as a weighted sum of four distinct cost components.

$$\begin{aligned} \min Z = & \sum_{f \in F} P_f^{Rej} (1 - Accept_f) + \sum_{f \in F} P_f^{Arr} D_f^{Arr} \\ & + \sum_{a \in A} P_a^{Dep} D_a^{Dep} + \varepsilon_p \sum_{f \in F} (X_f + Y_f) \end{aligned} \quad (1)$$

#### Explanation:

- **Rejection Cost:**  $\sum_{f \in F} P_f^{Rej} (1 - Accept_f)$ . This term imposes a penalty for each new service request  $f$  that is rejected. If  $Accept_f = 0$ , the term  $(1 - Accept_f)$  becomes 1, and the cost  $P_f^{Rej}$  is incurred.
- **Arrival Delay Cost:**  $\sum_{f \in F} P_f^{Arr} D_f^{Arr}$ . This component penalizes deviations from the planned schedule by calculating the cost of arrival delays for new aircraft.
- **Departure Delay Cost:**  $\sum_{a \in A} P_a^{Dep} D_a^{Dep}$ . Similarly, this term accounts for the cost associated with departure delays for all aircraft, both current and new.
- **Positioning Cost:**  $\varepsilon_p \sum_{f \in F} (X_f + Y_f)$ . This is a regularization term with a small coefficient  $\varepsilon_p$  that encourages the model to place new aircraft closer to the hangar's origin. This promotes a compact and organized spatial layout without overriding the primary cost considerations.

### 3.7. Model Constraints

Constraints define the rules and physical limitations of the system, ensuring that the solution is both feasible and realistic.

### 3.7.1. Acceptance and Scheduling Constraints

These constraints establish the fundamental relationships between the acceptance decision and the scheduling variables.

$$X_f + Y_f + Roll\_in_f + Roll\_out_f + D_f^{Arr} + D_f^{Dep} \leq (M_X + M_Y + 4M_T) \cdot Accept_f, \quad \forall f \in F \quad (2)$$

$$Roll\_in_f \geq ETA_f \cdot Accept_f, \quad \forall f \in F \quad (3)$$

$$Roll\_out_a - Roll\_in_a \geq ServT_a \cdot Accept_a, \quad \forall a \in A \quad (4)$$

$$D_f^{Arr} \geq Roll\_in_f - ETA_f, \quad \forall f \in F \quad (5)$$

$$D_a^{Dep} \geq Roll\_out_a - ETD_a, \quad \forall a \in A \quad (6)$$

#### Explanation:

- **Constraint (2):** A Big-M formulation that ensures if a new aircraft  $f$  is rejected ( $Accept_f = 0$ ), all associated continuous variables (position, time, and delay) are forced to be zero. If accepted ( $Accept_f = 1$ ), the constraint becomes non-binding.
- **Constraint (3):** An accepted aircraft cannot roll in before its Expected Time of Arrival (ETA).
- **Constraint (4):** The duration an accepted aircraft occupies a hangar spot must be sufficient to cover its required service time.
- **Constraint (5):** Defines the arrival delay for a new aircraft as the non-negative difference between its actual roll-in time and its ETA.
- **Constraint (6):** Defines the departure delay for any aircraft as the non-negative difference between its actual roll-out time and its ETD.

### 3.7.2. Hangar Physical and Non-overlapping Constraints

These constraints ensure that aircraft fit within the hangar boundaries and do not physically overlap.

$$X_f \geq Buffer \cdot Accept_f, \quad \forall f \in F \quad (7)$$

$$X_f + W_f \leq HW - Buffer + M_X(1 - Accept_f), \quad \forall f \in F \quad (8)$$

$$Y_f \geq Buffer \cdot Accept_f, \quad \forall f \in F \quad (9)$$

$$Y_f + L_f \leq HL - Buffer + M_Y(1 - Accept_f), \quad \forall f \in F \quad (10)$$

$$X_b + W_b + Buffer \leq X_a + M_X(1 - Right_{ab}), \quad \forall a, b \in A, a \neq b \quad (11)$$

$$Y_b + L_b + Buffer \leq Y_a + M_Y(1 - Above_{ab}), \quad \forall a, b \in A, a \neq b \quad (12)$$

#### Explanation:

- **Constraints (7) - (10):** These four constraints enforce that any accepted new aircraft is placed entirely within the hangar's usable area, maintaining the specified safety 'Buffer' from the walls.
- **Constraint (11):** This constraint, along with its counterpart for the Y-axis, prevents spatial overlap. If  $Right_{ab} = 1$ , it signifies that aircraft  $a$  is entirely to the right of aircraft  $b$ . The constraint then enforces that the X-coordinate of  $a$ 's left edge ( $X_a$ ) must be greater than or equal to the X-coordinate of  $b$ 's right edge ( $X_b + W_b$ ) plus the safety buffer. If  $Right_{ab} = 0$ , the Big-M term renders the constraint inactive.
- **Constraint (12):** This functions identically to the previous constraint but for the vertical (Y) axis, using the binary variable  $Above_{ab}$ .

### 3.7.3. Aircraft Separation and Relationship Constraints

These constraints establish the logical disjunctive relationships required to avoid conflicts between any pair of aircraft.

$$\begin{aligned} & Right_{ba} + Right_{ab} + Above_{ba} + Above_{ab} \\ & + OutIn_{ab} + OutIn_{ba} \geq Accept_a + Accept_b - 1, \end{aligned} \quad \forall a, b \in A, a < b \quad (13)$$

$$Roll\_out_a + \varepsilon_t \leq Roll\_in_b + M_T(1 - OutIn_{ab}), \quad \forall a, b \in A, a \neq b \quad (14)$$

$$\begin{aligned} & Roll\_in_g \geq Roll\_in_f + \varepsilon_t - M_T(1 - InIn_{fg}) \\ & - M_T(2 - Accept_f - Accept_g), \end{aligned} \quad \forall f, g \in F, f \neq g \quad (15)$$

$$\begin{aligned} & Roll\_in_f \geq Roll\_in_g + \varepsilon_t - M_T \cdot InIn_{fg} \\ & - M_T(2 - Accept_f - Accept_g), \end{aligned} \quad \forall f, g \in F, f \neq g \quad (16)$$

$$\begin{aligned} & Roll\_out_b \geq Roll\_out_a + \varepsilon_t - M_T(1 - OutOut_{ab}) \\ & - M_T(2 - Accept_a - Accept_b), \end{aligned} \quad \forall a, b \in A, a < b \quad (17)$$

$$\begin{aligned} & Roll\_out_a \geq Roll\_out_b + \varepsilon_t - M_T \cdot OutOut_{ab} \\ & - M_T(2 - Accept_a - Accept_b), \end{aligned} \quad \forall a, b \in A, a < b \quad (18)$$

$$\begin{aligned} & Roll\_out_b \geq Roll\_in_a + \varepsilon_t - M_T(1 - InOut_{ab}) \\ & - M_T(2 - Accept_a - Accept_b), \end{aligned} \quad (19)$$

$\forall a, b \in A, a \neq b$ , where  $a \in F \vee b \in F$

$$\begin{aligned} & Roll\_in_a \geq Roll\_out_b + \varepsilon_t - M_T \cdot InOut_{ab} \\ & - M_T(2 - Accept_a - Accept_b), \end{aligned} \quad (20)$$

$\forall a, b \in A, a \neq b$ , where  $a \in F \vee b \in F$

#### Explanation:

- **Constraint (13):** This is a generalized disjunctive constraint. It mandates that for any pair of accepted aircraft  $(a, b)$ , they must be separated in at least one dimension: spatially (one is right of, left of, above, or below the other) or temporally (one departs before the other arrives).

- **Constraint (14):** This constraint gives meaning to the  $OutIn_{ab}$  variable. If  $OutIn_{ab} = 1$ , it enforces that aircraft  $a$  must complete its roll-out at least  $\varepsilon_t$  time units before aircraft  $b$  can begin its roll-in.
- **Constraints (15) and (16):** This pair of constraints establishes a strict sequence for the roll-in times of any two new aircraft,  $f$  and  $g$ , if both are accepted. The binary variable  $InIn_{fg}$  acts as a switch: if  $InIn_{fg} = 1$ , constraint (16) forces  $f$  to roll-in before  $g$ ; if  $InIn_{fg} = 0$ , constraint (15) forces  $g$  to roll-in before  $f$ .
- **Constraints (17) and (18):** This pair works identically to the one above but enforces a strict sequence for the roll-out times of any two aircraft, preventing simultaneous departures.
- **Constraints (19) and (20):** This pair establishes a sequential relationship between the roll-in of one aircraft and the roll-out of another, using the binary variable  $InOut_{ab}$  to determine the order.

#### 3.7.4. Blocking Constraints

These constraints model simplified logistical pathways to prevent deadlocks where one aircraft's movement is obstructed by another. A simplified blocking scenario is illustrated in Figure 2.

$$\begin{aligned}
 Roll\_out_a &\geq Roll\_out_b + \varepsilon_t \\
 - M_T \cdot ((1 - Above_{ba}) + Right_{ab} + Right_{ba} \\
 + (1 - InIn_{ab})), &\quad \forall a, b \in A, a \neq b
 \end{aligned} \tag{21}$$

$$\begin{aligned}
 Roll\_in_a &\geq Roll\_out_b + \varepsilon_t \\
 - M_T \cdot ((1 - Above_{ba}) + Right_{ab} + Right_{ba} + InIn_{ab}), &\quad \forall a, b \in A, a \neq b, \text{ where } a \in F \vee b \in F
 \end{aligned} \tag{22}$$

#### Explanation:

- **Constraint (21) (Departure Blocking):** This constraint prevents a departure deadlock. Consider the scenario in Figure 2, where aircraft 'b' is positioned at a higher Y-coordinate than aircraft 'a', directly obstructing its path to the hangar exit. This situation is captured mathematically when 'b' is above 'a' ( $Above_{ba} = 1$ ), they are in the same vertical lane (neither is to the right or left of the other, so  $Right_{ab} = 0$

and  $Right_{ba} = 0$ ), and ‘a’ arrived before ‘b’ ( $InIn_{ab} = 1$ ). Under these specific conditions, the Big-M term in the constraint becomes zero, activating the rule  $Roll\_out_a \geq Roll\_out_b + \varepsilon_t$ . Using the example data from the figure, ‘b’’s departure ( $Roll\_out_b$ ) is scheduled at time 120. This rule forces ‘a’’s departure to occur after 120, creating a departure delay ( $D_a^{Dep}$ ) since its original  $ETD_a$  was 100. The model must then weigh the cost of this delay against other alternatives, such as placing ‘b’ in a non-blocking position.

- **Constraint (22) (Arrival Blocking):** This constraint handles a similar scenario for arrivals. Imagine aircraft ‘b’ is already parked as shown in Figure 2. If the model attempts to schedule a new aircraft ‘a’ to arrive and park in the position shown (below ‘b’), the same blocking condition exists ( $Above_{ba} = 1$ , same lane). The constraint activates, enforcing  $Roll\_in_a \geq Roll\_out_b + \varepsilon_t$ . This means ‘a’ is not allowed to enter the hangar until the blocking aircraft ‘b’ has departed, potentially causing a significant arrival delay ( $D_a^{Arr}$ ).

### 3.8. Initial Conditions and Variable Domains

#### 3.8.1. Fixed Initial Values

These constraints initialize the model based on the state of the hangar at the beginning of the planning horizon.

$$Accept_c = 1, \quad \forall c \in C \quad (23)$$

$$X_c = X_c^{init}, \quad \forall c \in C \quad (24)$$

$$Y_c = Y_c^{init}, \quad \forall c \in C \quad (25)$$

$$Roll\_in_c = 0, \quad \forall c \in C \quad (26)$$

$$InIn_{cf} = 1, \quad \forall c \in C, f \in F \quad (27)$$

$$InIn_{fc} = 0, \quad \forall f \in F, c \in C \quad (28)$$

$$InIn_{cd} = 1, \quad \forall c, d \in C, c \neq d \quad (29)$$

#### 3.8.2. Variable Type Definitions

$$X_a, Y_a, Roll\_in_a, Roll\_out_a, D_f^{Arr}, D_a^{Dep} \geq 0 \quad (30)$$

$$Accept_a, Right_{ab}, Above_{ab}, \dots \in \{0, 1\} \quad (31)$$

**Explanation:**

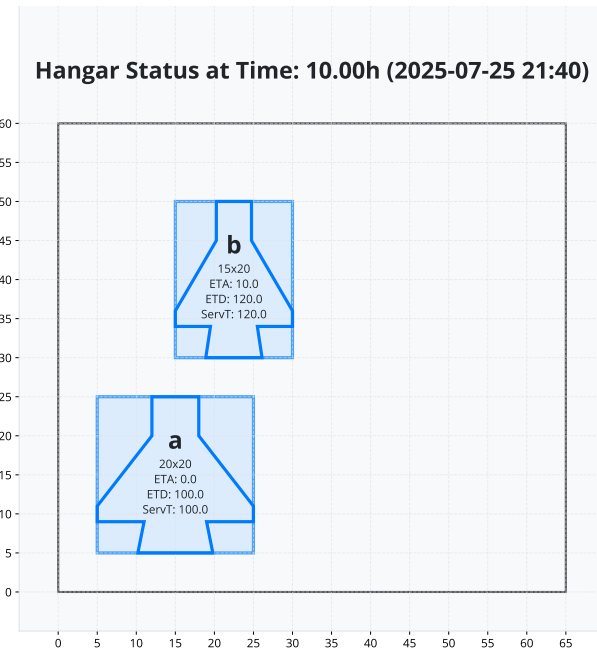


Figure 2: An illustration of a blocking scenario. Aircraft ‘b’ is parked at a higher Y-coordinate, obstructing aircraft ‘a’ from reaching the hangar exit (assumed at the top). For the departure case, this situation arises if ‘a’ arrived first and ‘b’ subsequently parked in the blocking position; consequently, ‘b’ must depart before ‘a’ can exit. For the arrival case, if ‘b’ is already present, ‘a’ cannot move into its depicted position until ‘b’ has departed.

- **Constraints (23)-(26):** These equations fix the status of aircraft already in the hangar: they are considered accepted, their positions are known, and their roll-in time is set to zero relative to the start of the plan.
- **Constraints (27)-(29):** These constraints pre-define the roll-in sequence to be consistent with reality: all current aircraft ( $c$ ) are considered to have rolled in before any future aircraft ( $f$ ). They also establish a fixed, albeit arbitrary, roll-in order among the current aircraft to satisfy sequencing logic.
- **Constraints (30) and (31):** These define the domains for the decision variables, ensuring continuous variables are non-negative and binary variables take values of 0 or 1.

## 4. Heuristic Solution Approach

While the MILP model guarantees optimality, its computational requirements can become significant for very large-scale instances or in time-critical operational contexts. To provide a performance benchmark and a rapid decision-making alternative, we developed an **Automated Constructive Heuristic (ACH)**. The purpose of the ACH is not to compete with sophisticated metaheuristics (e.g., genetic algorithms or simulated annealing), but rather to serve as a robust baseline that mimics a logical, priority-driven human planning process. By comparing the MILP’s optimal solutions against the outcomes of this fast, greedy approach, we can rigorously quantify the economic value of achieving true optimality.

### 4.1. Algorithm Design and Rationale

The ACH is a deterministic, single-pass constructive heuristic implemented in Python. It makes sequential, irrevocable decisions, building a feasible solution by processing one aircraft at a time. Its design is grounded in a set of logical rules that ensure every decision respects the core operational constraints defined in the mathematical model. This direct correspondence ensures that the heuristic produces physically and logically viable schedules that are directly comparable to the MILP solutions. The algorithm operates in two primary phases: prioritization and sequential placement.

#### 4.1.1. Phase 1: Prioritization Rule

The cornerstone of the heuristic is its prioritization logic, which determines the sequence in which new aircraft requests ( $f \in F$ ) are considered for placement. A well-defined priority queue is essential for a greedy algorithm, as the initial decisions heavily constrain subsequent options. All new aircraft are sorted into a priority list,  $L$ , based on the following lexicographical criteria, applied in order:

1. **Rejection Penalty ( $P_f^{Rej}$ )**: Descending order. Aircraft with higher rejection penalties are prioritized to minimize the most significant potential costs first. This reflects the high economic or strategic value of certain maintenance tasks.
2. **Expected Time of Arrival ( $ETA_f$ )**: Ascending order. Among aircraft with equal rejection penalties, those scheduled to arrive earlier are considered first. This rule aims to adhere to the original schedule as closely as possible.
3. **Service Time ( $ServT_f$ )**: Ascending order. As a final tie-breaker, aircraft requiring less time in the hangar are prioritized. This heuristic choice aims to increase hangar throughput by processing quicker tasks first, potentially freeing up space for subsequent, longer-duration jobs.

This multi-attribute rule creates a deterministic and operationally sensible sequence that guides the heuristic's greedy decisions.

#### 4.1.2. Phase 2: Sequential Placement and Scheduling

After establishing the priority list  $L$ , the algorithm iterates through it, attempting to find a feasible spatiotemporal slot for each aircraft. For a given aircraft, the heuristic initiates a search for a valid placement starting at its earliest possible roll-in time, which is its  $ETA_f$ . The search space is explored in two dimensions: time and space.

The core of this phase is the feasibility check for a potential placement. For a given coordinate pair  $(x, y)$  and a roll-in time  $t$ , this function rigorously validates the decision against the set of fixed, previously scheduled aircraft. It enforces the same critical constraints as the MILP model:

- **Hangar Boundaries:** The aircraft's footprint, including the safety 'Buffer', must be entirely within the hangar dimensions  $(HW, HL)$ .

- **Spatial Non-overlapping:** The new aircraft's buffered bounding box cannot overlap with that of any other aircraft already scheduled to be in the hangar during the same time interval.
- **Temporal Separation:** All roll-in and roll-out events must be separated by the minimum time gap,  $\varepsilon_t$ .
- **Blocking Rules:** The heuristic enforces path-blocking logic. An aircraft cannot be placed in a position that blocks the exit path of an already-parked aircraft, nor can it be scheduled to arrive in a position whose entrance path is blocked by an existing aircraft until that aircraft has departed.

If, at a given time  $t$ , one or more valid placements are found, the algorithm does not merely select the first one. Instead, it performs an exhaustive spatial scan of the entire hangar grid, collects all feasible positions into a candidate set, and then selects the best spot among them. The selection criterion is the minimization of the sum of coordinates  $(x + y)$ , a greedy choice that promotes a compact and organized layout by favoring positions closer to the hangar's origin.

If no valid placement is found at time  $t$ , the algorithm incrementally delays the potential roll-in time by a small step,  $\varepsilon_t$ , and re-evaluates the entire hangar space at the new time. This process continues until a feasible slot is identified or the potential arrival delay becomes economically unviable.

The decision to reject an aircraft is guided by a straightforward economic rationale: the search continues only as long as the cumulative cost of delaying its arrival is lower than the fixed penalty for rejection. To formalize this, the algorithm determines the economic break-even point, where the total delay cost equals the rejection penalty. This yields a threshold on the maximum allowable arrival delay,  $D_{max}^{Arr}$ , computed as follows:

$$D_{max}^{Arr} = \frac{P_f^{Rej}}{P_f^{Arr}}$$

Accordingly, the latest admissible arrival time,  $t_{max}$ , is the expected time of arrival ( $ETA_f$ ) plus this maximum delay:

$$t_{max} = ETA_f + \frac{P_f^{Rej}}{P_f^{Arr}}$$

The search for a valid spot is terminated and the aircraft is rejected if the search time  $t$  exceeds this calculated  $t_{max}$ . This mechanism provides a smart, cost-aware trade-off between delaying and rejecting service. The heuristic's logic is visualized in Figure 3.

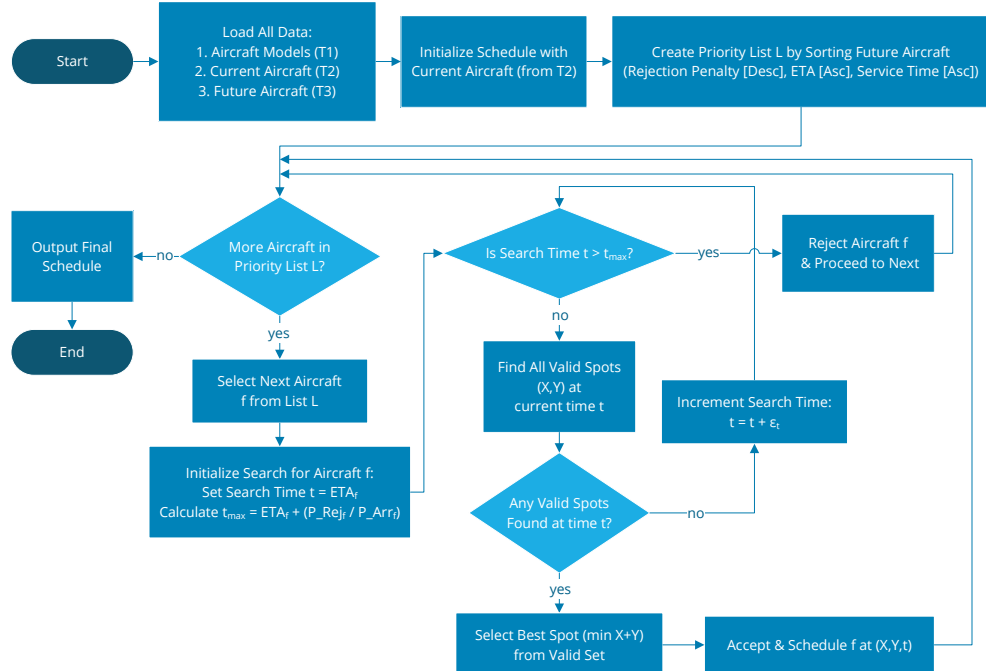


Figure 3: Flowchart of the Automated Constructive Heuristic (ACH). The "Valid Spot" check encapsulates all spatial, temporal, and blocking constraints, including hangar boundaries, non-overlapping rules, minimum time gaps, and path blocking logic.

## 5. Computational Study and Results

This section presents the results of our computational experiments, designed to evaluate the performance of the exact MILP model and the proposed heuristic approach.

### 5.1. Experimental Setup

All experiments were conducted on a machine with an Intel Core i7-10750H CPU @ 2.60GHz and 16 GB of RAM. The proposed MILP model was

implemented in GAMS and solved using the CPLEX solver. The Automated Constructive Heuristic (ACH) and the visualization tool were implemented in Python 3.13.

We tested the model using a specific set of operational parameters based on a representative hangar configuration. The hangar dimensions were set to a width (HW) of 65 meters and a length (HL) of 60 meters. A mandatory safety buffer of 5 meters was enforced between aircraft and between aircraft and the hangar walls. For temporal constraints, the minimum time gap between movements ( $\varepsilon_t$ ) was set to 0.1 hours (6 minutes). A small positioning penalty coefficient ( $\varepsilon_p$ ) of 0.001 was used to encourage a compact layout. It is important to note that these values are user-configurable parameters within the model, allowing for adaptation to different operational environments.

### 5.2. Test Instance Generation

To evaluate the performance of our proposed model, we developed a systematic procedure for generating realistic and reproducible test instances. The instances are named *Inst-N-V*, where  $N$  denotes the number of new aircraft requests and  $V$  is a version identifier. For each parameter type, the corresponding values across all aircraft were generated as independent and identically distributed (i.i.d.) random variables. In addition, the random variables associated with different parameter types (e.g., service time and arrival time) were assumed to be mutually independent.

The generation of temporal parameters was designed to ensure consistent operational density across different problem sizes. First, we defined a maximum arrival time,  $ETA_{max}$ , for each instance, calculated as  $ETA_{max} = N \times f_{TH}$ . Here,  $f_{TH}$  is the **Time Horizon Factor**, a constant set to 80 to proportionally expand the arrival window as the number of aircraft increases. The individual Estimated Times of Arrival ( $ETA_f$ ) were then drawn from a continuous uniform distribution over the interval  $[0, ETA_{max}]$ . The required service time for each aircraft,  $ServT_f$ , was similarly generated from  $U[100, 400]$  hours. Finally, the Expected Time of Departure ( $ETD_f$ ) was determined by the formula  $ETD_f = ETA_f + ServT_f + T_{buffer}$ , where the **Schedule Buffer Time**,  $T_{buffer}$ , was a random value from  $U[24, 72]$  hours.

To introduce realistic complexity, we incorporated two levels of heterogeneity:

1. **Physical Heterogeneity:** Each aircraft was randomly assigned one of eight physical models, corresponding to different geometric dimensions  $(W_f, L_f)$ , which creates complex spatial packing challenges.

2. **Economic Heterogeneity:** The economic value of each aircraft was differentiated through a two-step process. First, each aircraft was designated as a 'VIP' based on a **Bernoulli trial** with a success probability of 0.2. Second, penalty costs were assigned based on this status. Rejection penalties,  $P_f^{Rej}$ , were sampled from a discrete uniform distribution— $U\{1500, \dots, 2000\}$  for VIPs and  $U\{700, \dots, 1200\}$  for normal aircraft. Delay penalties, however, were deterministic: the per-hour costs for arrival and departure ( $P_f^{Arr}$ ,  $P_f^{Dep}$ ) were set to (10, 20) for normal aircraft and triple those values (30, 60) for VIPs.

This structured generation method allowed us to create a comprehensive testbed that realistically mimics the spatial, temporal, and economic trade-offs inherent in real-world hangar management.

### 5.3. Performance Analysis and Comparison

We conducted experiments on instances of varying sizes to evaluate the performance of the proposed MILP model and the ACH heuristic. Table 1 details the scale of the MILP formulation, showing a polynomial growth in variables and constraints as the number of future aircraft (N) increases. The comprehensive computational results are presented in Table 2, which forms the basis for the subsequent analysis.

The analysis of the results reveals a clear trade-off between solution quality and computational effort. The MILP model consistently finds provably optimal solutions (0% gap) for small to medium instances (N05 to N25) in remarkably short times. This highlights the efficiency of the continuous-time formulation for typical operational planning scenarios and represents a significant improvement over discrete-time models that struggle with similar sizes. However, as expected for an NP-hard problem, the time required to prove optimality grows exponentially with problem size. For the largest instance, N40, reaching the optimal solution required approximately 4.2 hours. While substantial, this ability to solve a large, complex instance to proven optimality is a major achievement of our formulation.

To better visualize these trade-offs, we first compare the total operational cost of the optimal MILP solutions against those from the ACH heuristic in Figure 4. The chart visually confirms the significant cost savings achieved by the exact model, as quantified by the "Gap vs Opt (%)" column in Table 2. The performance gap widens as the problem scale increases, underscoring the substantial economic value of optimal planning over the myopic, greedy

decisions of the simple heuristic. Next, Figure 5 illustrates the computational time disparity. Using a dual-axis plot with a logarithmic scale for the MILP’s solution time, it starkly contrasts the exponential growth of the exact method with the near-linear, low computational footprint of the heuristic. This figure encapsulates the core challenge: the pursuit of optimality comes at a high computational cost for large-scale problems.

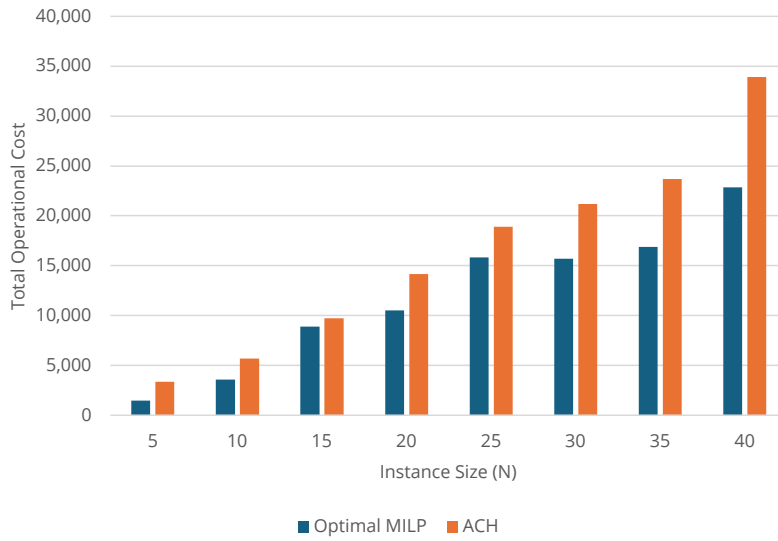


Figure 4: Comparison of total operational cost between the optimal MILP solution and the ACH heuristic. The chart illustrates the significant cost savings achieved by the exact optimization model, highlighting the economic value of optimal planning over simple heuristics.

This raises a critical question for practical implementation: is the long wait for a guaranteed optimal solution always necessary? Figure 6 provides the answer. By focusing on the larger instances (N30, N35, N40), this chart demonstrates the MILP solver’s ability to deliver high-quality, near-optimal solutions in a fraction of the time. For instance, in the N40 case, a solution guaranteed to be within 10% of the optimum is found in approximately 1.4 hours (4,960 s), while a 5% gap solution is found in 2.7 hours (9,726 s)—significant reductions from the 4.2 hours (15,033 s) needed for the proven optimum. This demonstrates the model’s strategic flexibility. For long-term, strategic planning, investing the time to find a guaranteed optimal solution is justified. For more time-sensitive, operational decisions, managers can terminate the solver early to obtain a high-quality solution with a known quality

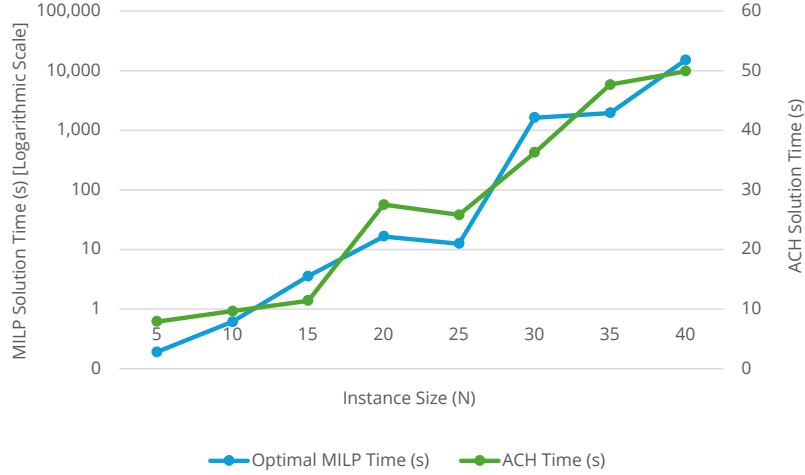


Figure 5: Computational time as a function of problem size. The dual-axis chart displays the solution time for the optimal MILP model (primary Y-axis, logarithmic scale) and the ACH heuristic (secondary Y-axis), highlighting the trade-off between optimality and speed.

bound, making the model a versatile and practical tool for real-world MRO environments.

Table 1: Specifications of the MILP model for the generated test instances.

Instance	N (Future Aircraft)	MILP Model Data		
		All Variables	Binary Variables	Constraints
N05	5	277	212	441
N10	10	807	692	1,391
N15	15	1,612	1,447	2,866
N20	20	2,692	2,477	4,866
N25	25	4,047	3,782	7,391
N30	30	5,677	5,362	10,441
N35	35	7,582	7,217	14,016
N40	40	9,762	9,347	18,116

Table 2: Computational results comparing the performance of MILP (at different optimality gaps) and ACH.

Instance	MILP (GAMS by CPLEX Solver)						ACH		
	0% Gap		5% Gap		10% Gap		Total Cost <sup>1</sup>	Time Cost <sup>1</sup>	Time
	Total Cost <sup>1</sup>	Time (s)	Total Cost <sup>1</sup>	Time (s)	Total Cost <sup>1</sup>	Time (s)			
N05	1,496	0	1,496	0	1,496	0	3,376	8	126%
N10	3,567	1	3,567	1	3,567	1	5,679	10	59%
N15	8,896	4	8,896	4	8,896	4	9,737	11	9%
N20	10,531	17	10,531	13	10,531	10	14,147	28	34%
N25	15,833	12	15,833	10	16,331	10	18,910	26	19%
N30	15,700	1,618	15,700	577	15,700	193	21,166	36	35%
N35	16,884	1,950	16,931	686	17,082	367	23,701	48	40%
N40	22,829	15,033	22,830	9,726	22,829	4,960	33,910	50	49%

<sup>1</sup>The reported Total Cost primarily includes penalties for rejections and delays. The minor positioning cost term, used as a regularization factor in the objective function, has a negligible impact on the total value and is excluded for clarity.

<sup>2</sup>Calculated against the optimal solution found by MILP (0% Gap).

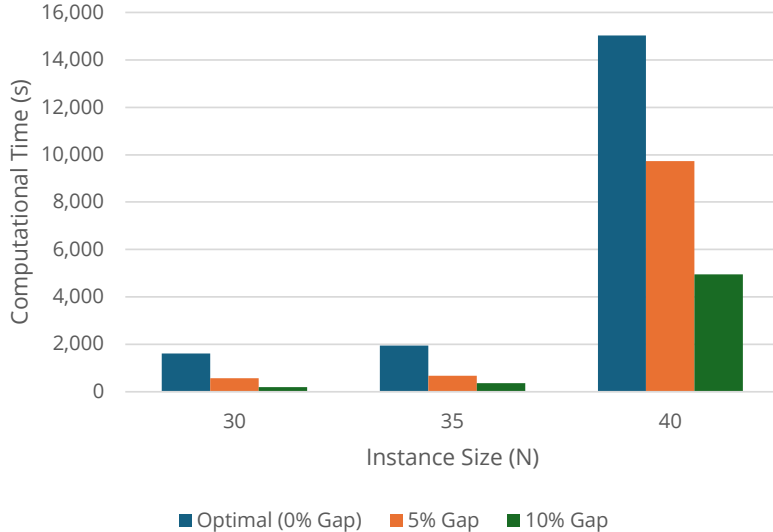


Figure 6: Computational time required to achieve different solution quality levels for large-scale instances (N30, N35, N40). The results demonstrate the model’s flexibility, allowing managers to trade computational effort for a known optimality gap.

#### 5.4. Robustness to Event Congestion

A critical limitation of event-based formulations, as highlighted in our literature review with respect to Qin et al. (2019), is their performance sensitivity not just to the number of aircraft, but to the temporal density of events. A highly congested schedule can lead to a massive increase in possible scheduling combinations, which severely slows down the solution process. To demonstrate the inherent robustness of our continuous-time formulation against this challenge, we designed a controlled, two-stage computational experiment based on the N15 instance. The objective is to empirically validate that our model’s complexity is primarily driven by the number of entities (aircraft), not by the congestion of their arrival times.

##### 5.4.1. Stage 1: Validating the Model’s Economic Rationality (N15-C)

First, we created a "congested" scenario, denoted as N15-C, by modifying the N15 instance. We systematically reduced the time windows between consecutive Expected Times of Arrival (ETAs), forcing a high degree of temporal overlap among service requests. The rejection penalties ( $P_f^{Rej}$ ) were kept identical to the base scenario.

As shown in Table 3, the model’s response was both swift and economically rational. Faced with a highly complex scheduling problem, the solver found an optimal solution in just 1 second by rejecting 9 aircraft—two more than in the base case. This outcome confirms that, when economically permissible, the model intelligently avoids unnecessary complexity by rejecting requests that would induce high systemic costs, thus validating its core logic. This test serves as a crucial control, demonstrating that without sufficient economic incentive, the model will not engage with the induced complexity.

#### *5.4.2. Stage 2: Assessing Performance under Forced Complexity (N15-C+)*

Next, to truly test the model’s capability to manage intricate spatiotemporal conflicts, we created the N15-C+ instance. We used the same congested arrival schedule as in N15-C but significantly increased the rejection penalties. This change forced the model to accept a high number of aircraft, thereby preventing it from circumventing the congestion and compelling it to find a feasible, albeit complex, schedule.

The results from this stage are the central finding of this analysis. Despite the severe operational constraints, the model successfully found an optimal solution that accepted the same number of aircraft as the non-congested N15 scenario (rejecting only 7). To achieve this, it orchestrated a highly sophisticated schedule involving significant, strategic delays. For example, it postponed the arrival of aircraft a03 and a05 by over 118 and 98 hours, respectively, creating a cascading effect of departure delays to resolve numerous spatial and temporal conflicts.

Most importantly, the time required to solve this highly complex and constrained problem was merely 2 seconds. This is remarkably close to the 4 seconds needed for the standard, non-congested N15 instance.

#### *5.4.3. Conclusion of the Experiment*

This two-stage experiment provides compelling evidence that the computational performance of our continuous-time MILP model is remarkably insensitive to event density. Unlike event-based models that falter when faced with temporal congestion, our formulation’s solution time remains stable and primarily dependent on the number of aircraft. This demonstrated insensitivity to event density highlights a fundamental advantage of the proposed continuous-time approach, particularly when compared to event-based models whose performance is known to degrade under such temporal congestion.

Table 3: Analysis of Model Performance under Congestion for the N15 Instance.

Instance	Scenario Description	Rejection Penalty Level	Aircraft Rejected	Total Cost	Solution Time (s)
N15	Standard	Normal	7	8,896	4
N15-C	Congested ETAs	Normal	9	10,524	1
N15-C+	Congested ETAs	High	7	41,595	2

### 5.5. Managerial Insights

The computational results and their analysis provide several actionable insights for hangar managers, highlighting the practical value of the proposed optimization framework.

- **The Value of Optimal, Non-Intuitive Decisions:** A key insight is that the MILP model makes counter-intuitive yet globally optimal decisions. For instance, the model may choose to reject a high-priority aircraft (with a large rejection penalty) or impose a strategic delay on another, if doing so prevents a cascade of costly conflicts and unlocks a more profitable overall schedule. Such complex, system-wide trade-offs are difficult for human planners or simple heuristics to identify, demonstrating that an exact optimization model can uncover hidden costs and opportunities.
- **Strategic Flexibility: Trading Optimality for Speed:** The analysis in Figure 6 directly translates into a powerful managerial tool. Instead of a binary choice between a fast, suboptimal heuristic and a slow, optimal model, our approach offers a spectrum of solutions. Managers can now make informed decisions based on the operational context: for strategic, long-range planning where cost minimization is paramount, they can run the solver to optimality. For tactical, day-to-day scheduling where a quick, high-quality plan is needed, they can set an acceptable optimality gap (e.g., 5% or 10%) to receive a solution with a known quality guarantee in a fraction of the time.
- **Quantifying the Cost of Heuristics:** The significant performance gap between the MILP and ACH solutions (Figure 4) provides a clear financial justification for investing in advanced optimization tools. While heuristics are valuable for their speed, their myopic nature can lead to

substantially higher operational costs. Our study quantifies this difference, enabling organizations to perform a cost-benefit analysis of adopting a more sophisticated decision support system.

### 5.6. Solution Visualization

To bridge the gap between the model’s numerical output and practical application, a custom visualization tool was developed in Python. This tool serves as an interactive and dynamic decision support dashboard, translating the complex spatiotemporal solution into an intuitive graphical interface for hangar managers. Key features include a 2D animated layout of the hangar, an interactive timeline to step through events, and synchronized data tables.

This tool is not merely for presentation; it is a powerful analytical instrument. As illustrated in Figure 7, it provides managers with a clear snapshot of the hangar’s state at any point in time, enabling them to anticipate bottlenecks and understand the logic behind the optimal plan. The ability to visualize the intricate scheduling of movements—where the departure of one aircraft is precisely timed to clear a path for another—offers valuable managerial insights into the efficiency gains achievable through optimization. This transforms the abstract model into a tangible and actionable operational plan.

## 6. Conclusion and Future Work

This paper presented a novel continuous-time MILP model for the aircraft hangar spatial-temporal optimization problem, demonstrating significant computational advantages over previous discrete-time and event-based formulations. A comparative study against a constructive heuristic validated the substantial economic value of the exact model and yielded crucial insights into the trade-offs between solution quality and computational speed. Crucially, our study demonstrates that the proposed continuous-time formulation is remarkably robust to temporal event congestion—a known bottleneck for event-based models—thereby offering a more reliable and scalable solution for real-world dynamic environments.

The practical value of this optimization framework is further enhanced by the complementary visualization tool, which transforms the abstract numerical solution into a tangible and actionable operational plan. As derived from the computational results, the managerial insights confirm that such an optimization-based decision support system can guide managers toward

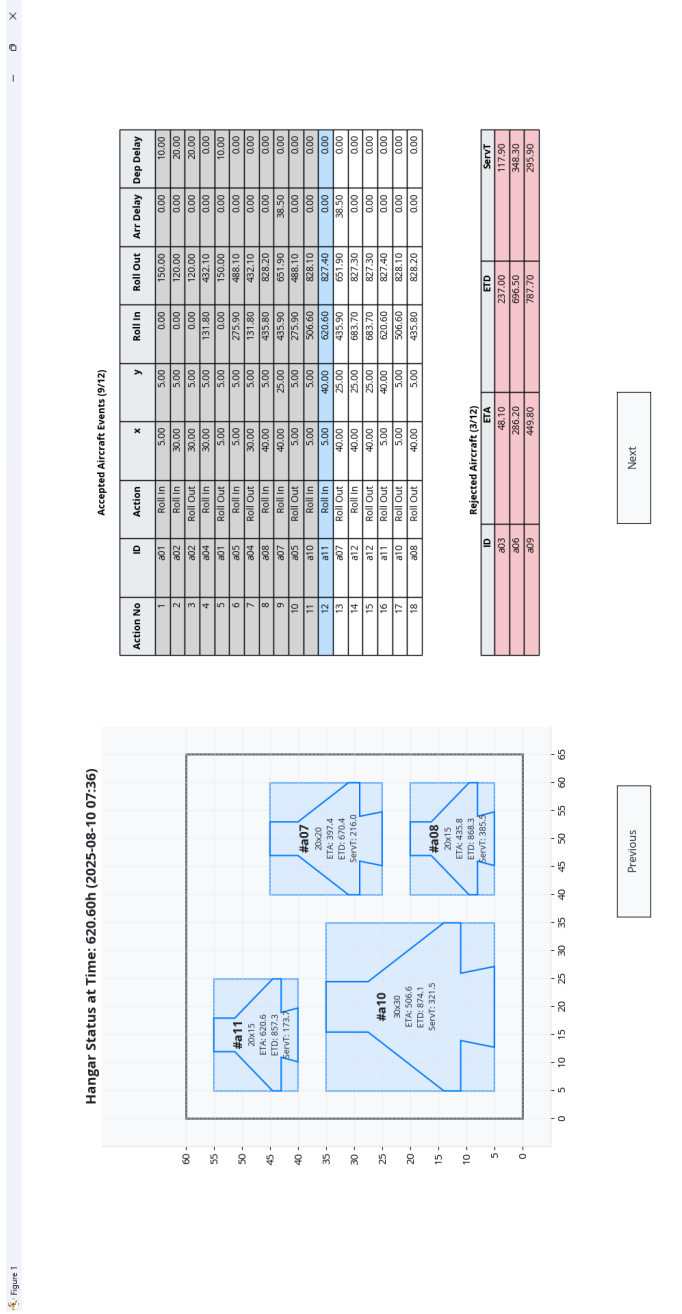


Figure 7: A snapshot from the custom decision support and visualization tool, simulating a desktop application window. The interface displays the optimal hangar configuration for the N10 test instance at time  $t=620.60h$ . The left panel shows the spatial layout of accepted aircraft, while the tables on the right provide detailed scheduling information for all accepted and rejected maintenance requests.

superior, often counter-intuitive, decisions that result in significant cost savings.

Future research could extend this model in several directions. Incorporating uncertainty, such as variable service times or unexpected arrivals, using stochastic programming or robust optimization techniques would enhance the model's real-world applicability. Furthermore, applying a rolling horizon framework to our continuous-time model presents a compelling avenue for future work. This approach could drastically reduce computation times for very large-scale or dynamic scenarios, and our model's inherent ability to handle an initial hangar state makes it particularly well-suited for such an implementation. More sophisticated, path-based blocking constraints could also be developed to model complex hangar layouts and movement paths more accurately. Finally, enhancing the automated heuristic with a dynamic, look-back mechanism or other metaheuristic improvement phases (e.g., local search) could help close the performance gap while maintaining low computational times.

### **Declaration of Competing Interest**

The authors declare that they have no known competing financial interests or personal relationships that could have appeared to influence the work reported in this paper.

### **CRediT authorship contribution statement**

**Shayan Farhang Pazhooh:** Conceptualization, Methodology, Software, Data Curation, Formal analysis, Validation, Investigation, Writing – original draft, Writing – review & editing, Visualization.

**Hossein Shams Shemirani:** Conceptualization, Methodology, Validation, Supervision, Project administration, Writing – review & editing.

### **Declaration of Generative AI and AI-assisted Technologies in the Writing Process**

During the preparation of this work the author(s) used Gemini (a large language model by Google) in order to assist with language refinement and editing. After using this tool, the author(s) reviewed and edited the content as needed and take full responsibility for the content of the published article.

## Funding

This research did not receive any specific grant from funding agencies in the public, commercial, or not-for-profit sectors.

## Data Availability Statement

The data and source codes that support the findings of this study are openly available in Zenodo at <https://doi.org/10.5281/zenodo.16734268>. The development repository is also available on GitHub at <https://github.com/shayanfp/Hangar-Model-Research>.

## References

Andrade, P., Silva, C., Ribeiro, B., Santos, B.F., 2021. Aircraft maintenance check scheduling using reinforcement learning. *Aerospace* 8, 113. doi:10.3390/aerospace8040113.

Arts, J., Boute, R.N., Loeys, S., van Staden, H.E., 2025. Fifty years of maintenance optimization: Reflections and perspectives. *European Journal of Operational Research* 322, 725–739. doi:10.1016/j.ejor.2024.07.002.

Belien, J., Cardoen, B., Demeulemeester, E., 2012. Improving workforce scheduling of aircraft line maintenance at sabena technics. *Interfaces* 42, 352–364. doi:10.2139/ssrn.1978728.

Chen, G., He, W., Leung, L.C., Lan, T., Han, Y., 2017. Assigning licenced technicians to maintenance tasks at aircraft maintenance base: a bi-objective approach and a chinese airline application. *International Journal of Production Research* 55, 5550–5563. doi:10.1080/00207543.2017.1296204.

Deng, Q., Santos, B.F., 2022. Lookahead approximate dynamic programming for stochastic aircraft maintenance check scheduling optimization. *European Journal of Operational Research* 299, 814–833. doi:10.1016/j.ejor.2021.09.019.

Gavranis, A., Kozanidis, G., 2015. An exact solution algorithm for maximizing the fleet availability of a unit of aircraft subject to flight and maintenance requirements. *European Journal of Operational Research* 242, 631–643. doi:10.1016/j.ejor.2014.10.016.

Guan, H., Wang, M., Meng, Q., 2025. Syncrolift dry dock scheduling with a capacitated ship transfer system. *Computers & Operations Research* 182, 107138. doi:10.1016/j.cor.2025.107138.

Jiang, H., Zeng, W., Wei, W., Tan, X., 2024. A bilevel flight collaborative scheduling model with traffic scenario adaptation: An arrival prior perspective. *Computers & Operations Research* 161, 106431. doi:10.1016/j.cor.2023.106431.

Jiang, Z., Liu, Z., Zhou, Z., Huang, Y., Li, J., 2025. Operations routing and scheduling problem: Concept, graphing and notation systems. *Computers & Operations Research* 177, 106992. doi:10.1016/j.cor.2025.106992.

de Jonge, B., Scarf, P.A., 2020. A review on maintenance optimization. *European Journal of Operational Research* 285, 805–824. doi:10.1016/j.ejor.2019.09.047.

van Kessel, P.J., Freeman, F.C., Santos, B.F., 2023. Airline maintenance task rescheduling in a disruptive environment. *European Journal of Operational Research* 308, 605–621. doi:10.1016/j.ejor.2022.11.017.

Liu, G., Guo, R., Chen, J., 2023. A scheduling model of civil aircraft maintenance stand based on spatiotemporal constraints. *Aircraft Engineering and Aerospace Technology* 95, 1518–1530. doi:10.1108/AEAT-11-2022-0330.

Liu, X., Chen, Z., Zhu, F., Chen, H., 2025. Study on static and dynamic performance of aircraft maintenance hangar under multiple load combinations. *PLOS ONE* 20, e0327195. doi:10.1371/journal.pone.0327195.

Niu, B., Cai, G., Zhou, T., 2025. Two-stage metaheuristic framework based on irregular contours matching for outsourced aircraft maintenance parking stand allocation problem. *IEEE Transactions on Automation Science and Engineering* 22, 6967–6983. doi:10.1109/TASE.2024.3457773.

Qin, Y., Chan, F.T., Chung, S., Qu, T., Niu, B., 2018. Aircraft parking stand allocation problem with safety consideration for independent hangar maintenance service providers. *Computers & Operations Research* 91, 225–236. doi:10.1016/j.cor.2017.10.001.

Qin, Y., Ng, K.K., Sun, X., 2024. Service accessibility strategy for aircraft maintenance routing with interorganizational collaborations on outsourcing maintenance. *Computers & Industrial Engineering* 190, 110071. doi:10.1016/j.cie.2024.110071.

Qin, Y., Wang, Z.X., Chan, F.T., Chung, S., Qu, T., 2019. A mathematical model and algorithms for the aircraft hangar maintenance scheduling problem. *Applied Mathematical Modelling* 67, 491–509. doi:10.1016/j.apm.2018.11.008.

Qin, Y., Zhang, J., Chan, F.T., Chung, S., Niu, B., Qu, T., 2020. A two-stage optimization approach for aircraft hangar maintenance planning and staff assignment problems under mro outsourcing mode. *Computers & Industrial Engineering* 146, 106607. doi:10.1016/j.cie.2020.106607.

Sriram, C., Haghani, A., 2003. An optimization model for aircraft maintenance scheduling and re-assignment. *Transportation Research Part A: Policy and Practice* 37, 29–48. doi:10.1016/S0965-8564(02)00004-6.

Witteman, M., Deng, Q., Santos, B.F., 2021. A bin packing approach to solve the aircraft maintenance task allocation problem. *European Journal of Operational Research* 294, 365–376. doi:10.1016/j.ejor.2021.01.027.

Zhang, X., Wang, X., Dong, W., Xu, G., 2025. Adaptive large neighborhood search for autonomous electric vehicle scheduling in airport baggage transport service. *Computers & Operations Research* 182, 107086. doi:10.1016/j.cor.2025.107086.